EUROPHYSICS LETTERS 15 April 2005

Europhys. Lett., **70** (2), pp. 225–231 (2005)
DOI: 10.1209/epl/i2004-10480-2

Infrared properties of electron-doped cuprates: Tracking normal-state gaps and quantum critical behavior in $Pr_{2-x}Ce_xCuO_4$

A. Zimmers[1], J. M. Tomczak[1], R. P. S. M. Lobo[1](*), N. Bontemps[1], C. P. Hill[2], M. C. Barr[2], Y. Dagan[2], R. L. Greene[2], A. J. Millis[3] and C. C. Homes[4]

[1] *Laboratoire de Physique du Solide (UPR 5 CNRS) ESPCI 10 rue Vauquelin, 75005 Paris, France*
[2] *Center for Superconductivity Research, Department of Physics University of Maryland - College Park, MD 20742, USA*
[3] *Physics Department, Columbia University - New York, NY 10027, USA*
[4] *Department of Physics, Brookhaven National Laboratory Upton, NY 11973, USA*

received 30 November 2004; accepted in final form 25 February 2005
published online 18 March 2005

PACS. 74.25.Gz – Optical properties.
PACS. 74.72.Jt – Other cuprates, including Tl and Hg-based cuprates.
PACS. 75.30.Fv – Spin-density waves.

Abstract. – We report the temperature dependence of the infrared-visible conductivity of $Pr_{2-x}Ce_xCuO_4$ thin films. When varying the doping from a non-superconducting film ($x = 0.11$) to a superconducting overdoped film ($x = 0.17$), we observe, up to optimal doping ($x = 0.15$), a *partial* gap opening. The magnitude of this gap extrapolates to zero for $x \sim 0.17$. A model combining a spin density wave gap and a frequency- and temperature-dependent self-energy reproduces our data reasonably well, suggesting the coexistence of magnetism and superconductivity in this material and the existence of a quantum critical point at this Ce concentration.

Over the last 15 years, significant work has been done on the differences and similarities between electron- and hole-doped cuprates. The two material families share a structure with CuO_2 planes, both exhibit superconductivity in a moderate doping range and both exhibit anomalous "normal" (non-superconducting) states characterized in some doping and temperature ranges by a normal-state gap.

In hole-doped materials early evidence for a normal-state gap ("pseudogap") came from nuclear magnetic resonance experiments [1, 2]. Angle-resolved photoemission (ARPES) experiments performed on the Bi-2212 material show that the pseudogap opens along the $(0, \pi)$ direction in k space [3] and evolves smoothly into the superconducting gap as the temperature T is lowered. However, in the hole-doped materials gap-like features do not appear in

(*) E-mail: lobo@espci.fr

the in-plane optical conductivity. The pseudogap is only observed as a decrease in the optically defined scattering rate [4, 5] instead of the suppression of low-frequency spectral weight observed in conventional density wave systems [6, 7].

On the electron-doped side, the most studied material is $Nd_{2-x}Ce_xCuO_4$ (NCCO) [8, 9]. The optical conductivity of non-superconducting single crystals ($x = 0$ to 0.125) shows a temperature-dependent high-energy feature which Onose *et al.* [10] associate with antiferromagnetic order or correlation (other authors have different interpretations [9, 11]). This compound is known to have commensurate (π, π) antiferromagnetic order for a wide range of doping from $x = 0$ to approximately 0.15. In this material, it is believed that superconductivity and magnetism do not coexist. ARPES measurements mapping the Fermi surface at low temperature find that intensity is suppressed where the nominal Fermi surface crosses the magnetic Brillouin zone boundary [12], also indicating a coupling of magnetism and electronic degrees of freedom.

In this letter we report measurements of the temperature evolution of the optical conductivity in a set of $Pr_{2-x}Ce_xCuO_4$ (PCCO) thin films. The PCCO material has a wider superconducting range than does NCCO. The magnetic phase diagram of $Pr_{2-x}Ce_xCuO_4$ has not been determined but in the related material $Pr_{1-x}LaCe_xCuO_4$, Fujita *et al.* [13] have found a transition from magnetism to superconductivity at $x \approx 0.1$. Thin films are extremely homogeneous in the Ce concentration and are easier to anneal than crystals. Most important, they can be made superconducting in the underdoped regime, whereas this seems difficult for crystals [10]. Our new generation of films are large enough to allow accurate optical studies, enabling us to track the optical behavior to low-energy scales ($\sim 2\,\mathrm{meV}$) and into the superconducting state [14]. Our data reveals the onset of a "high energy" partial gap below a characteristic temperature T_W which evolves smoothly with doping. The gap is directly evident in the measured optical conductivity for $x = 0.11$ and 0.13, it is absent down to 5 K for $x = 0.17$ and it has a subtle signature for $x = 0.15$ (optimal doping). It is present in two of our superconducting samples (0.13 and 0.15) in contrast to ref. [10] in which a gap feature was observed only in non-superconducting samples. The closure of the gap suggests a quantum critical point (QCP) around $x = 0.17$, consistent with transport evidence on similar samples [15]. We suggest that this gap originates from a spin density wave (SDW), consistent with ARPES [12], and that the QCP is an antiferromagnetic-paramagnetic one. We present arguments that this is not due to a two-phase coexistence.

The thin films studied in this work were epitaxially grown by pulsed-laser deposition on a $SrTiO_3$ substrate [16]. The samples studied are i) $x = 0.11$, not superconducting down to 4 K (thickness 2890 Å), ii) $x = 0.13$ (underdoped), $T_c = 15\,\mathrm{K}$ (thickness 3070 Å), iii) $x = 0.15$ (optimally doped), $T_c = 21\,\mathrm{K}$ (thickness 3780 Å), iv) $x = 0.17$ (overdoped); $T_c = 15\,\mathrm{K}$ (thickness 3750 Å). T_c for all the films were obtained by electrical resistance measurements (zero resistivity). Infrared-visible reflectivity spectra were measured for all samples in the 25–21000 cm^{-1} spectral range with a Bruker IFS 66 v Fourier Transform spectrometer within an accuracy of 0.2%. Data were taken at typically 12 temperatures (controlled better than 0.2 K) between 25 K and 300 K. The far-infrared (10–100 cm^{-1}) was measured for samples iii) and iv), utilizing a Bruker IFS 113 v at Brookhaven National Laboratory.

Figure 1 shows the raw reflectivity from 25 to 5000 cm^{-1} for a set of selected temperatures. As the temperature decreases, a suppression of R becomes conspicuous for $x = 0.11$ and 0.13 and is visible for $x = 0.15$ as a bending of the lowest temperature curve. Conversely, the reflectivity of the $x = 0.17$ sample increases monotonically with decreasing temperature over the whole spectral range shown. We applied a standard thin film fitting procedure to extract the optical conductivity from this data set [5, 17]. The real part $\sigma_1(\omega)$ of the optical

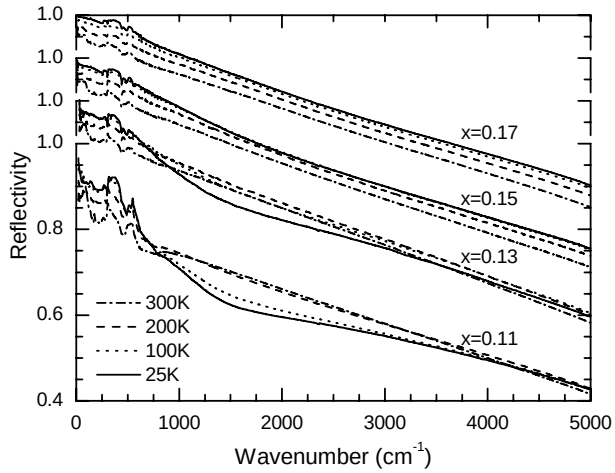

Fig. 1 – Raw infrared reflectivity of $x = 0.11$, 0.13, 0.15 and 0.17 samples. Curves for different concentrations are shifted from one another by 0.1 for clarity.

conductivity is plotted in fig. 2 (left panels). At low energy, for all concentrations, there is a Drude-like contribution which narrows as the temperature is lowered in the normal state from 300 K to 25 K. This implies a transfer of spectral weight, from higher (*e.g.*, $\gtrsim 1700\,\mathrm{cm}^{-1}$ for $x = 0.13$) to lower frequencies. Above $1000\,\mathrm{cm}^{-1}$, the feature noticed in the raw reflectivity

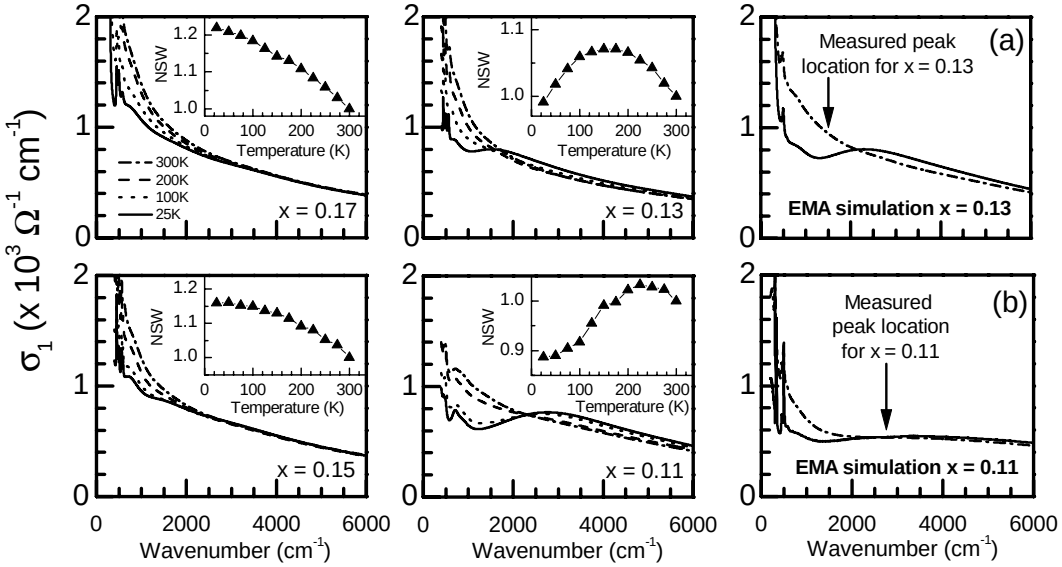

Fig. 2 – Left panels: real part of the optical conductivity from 400 to $6000\,\mathrm{cm}^{-1}$. The inset in each panel shows the normalized spectral weight $RSW(0, 2000\,\mathrm{cm}^{-1}, T)/RSW(0, 2000\,\mathrm{cm}^{-1}, 300\,\mathrm{K})$ plotted *vs.* temperature for upper cut-off frequency $\omega_H = 2000\,\mathrm{cm}^{-1}$. Right panels (a) and (b): Effective medium approximation (EMA) simulations of conductivity. Panel (a): attempts to simulate conductivity of $x = 0.13$ sample by combinations of $x = 0.11$ and $x = 0.17$. Panel (b): attempts to simulate $x = 0.11$ crystal by combinations of non-doped and $x = 0.17$ conductivities. The proportions of each phase were chosen so that the average Ce concentration is the nominal one.

for $x = 0.11$ and 0.13 produces a dip/hump structure. $\sigma_1(\omega)$ peaks around $\Omega_{Max} = 2750\,\mathrm{cm}^{-1}$ for $x = 0.11$ and around $\Omega_{Max} = 1500\,\mathrm{cm}^{-1}$ for $x = 0.13$. A similar feature was observed in NCCO single crystals only for doping levels where such crystals are *not superconducting* [10], in contrast to our observation in the $x = 0.13$ sample.

Homogeneity issues are a key question in cuprates [18]. We investigated the homogeneity of our samples in several ways. Using the X-ray analysis of an EDAX system, we verified that the $x = 0.15$ sample did not present any trace of inhomogeneity on the micron scale in the Pr, Ce or Cu concentrations. We also used the standard Bruggeman effective medium approximation [19] (valid for inhomogeneities smaller than the wavelength but larger than the mean free path of $\lesssim 50\,\text{Å}$) to investigate the possibility that the gap features observed in one concentration could arise from an inhomogeneous mixture of two different concentrations. The panel (b) of fig. 2 shows results of an attempt to simulate the optical conductivity of the $x = 0.11$ sample as a combination of 35% $x = 0$ [20] and 65% $x = 0.17$, as suggested in ref. [21]. The failure to describe the spectral-weight shift and peak development is evident. The panel (a) of fig. 2 shows results of an attempt to simulate the $x = 0.13$ sample from the $x = 0.11$ and $x = 0.17$ ones. For no parameters were we able to place the peak in σ_1 at the correct location. These, and other simulations (not shown) lead us to believe that the structures we observe are intrinsic.

We now present a spectral-weight analysis which shows that the features seen in σ_1 and R are due to the opening of a partial gap. We define the restricted spectral weight $RSW(\omega_L, \omega_H, T)$ via

$$RSW(\omega_L, \omega_H, T) = \frac{2}{\pi} \int_{\omega_L}^{\omega_H} \sigma_1(\omega, T) \mathrm{d}\omega. \tag{1}$$

The familiar f-sum rule implies $RSW(0, \infty, T) = ne^2/m$; the partial integrals provide insight into the rearrangement of the conductivity with temperature. In a conventional metal the conductivity is described by a "Drude peak" centered at $\omega = 0$ and with half width Γ decreasing as T is lowered. In this case, spectral weight is transferred from high to low energies as T decreases. On the other hand, the opening of a density wave gap leads to a transfer of spectral weight to higher energies, beyond the gap edge.

In all of our samples, $RSW(0, 20000\,\mathrm{cm}^{-1}, T)$ is temperature independent within 3%; however, the partial integrals display an informative T-dependence. The insets to fig. 2 display $RSW(0, 2000\,\mathrm{cm}^{-1}, T)$ normalized to the $T = 300\,\mathrm{K}$ values. The presence of a narrow Drude peak ($\lesssim 100\,\mathrm{cm}^{-1}$) implies that accurate low-frequency data (measured down to $10\,\mathrm{cm}^{-1}$) is important in order to get reliable zero-frequency extrapolations. The $x = 0.17$ curves display the steady increase in the normalized spectral weight expected of a Drude metal. On the other hand, both the $x = 0.11$ and $x = 0.13$ samples display a non-monotonic behavior indicating an upward shift of spectral weight beginning below $T \approx 225\,\mathrm{K}$ ($x = 0.11$) and $T \approx 150\,\mathrm{K}$ ($x = 0.13$); however, we note that all samples remain metallic at low temperatures as indicated by the presence of a Drude peak. In drawing this conclusion, it is important to integrate down to zero to insure that the weight is not transferred downwards into a narrow Drude peak. We believe that the only consistent interpretation of these data is that as T is lowered a gap appears on *part* of the Fermi surface. In particular, simulations of two component (Drude and mid-infrared) models, such as the polaron model of Lupi *et al.* [11] leads to negligible upwards transfer of spectral weight ($\sim 5\%$ of observed values).

To address the issue of the existence of a partial gap in the $x = 0.15$ (optimally doped) sample we compare in fig. 3 the RSW of $x = 0.13$, 0.15 and 0.17 in two frequency ranges. For clarity, each curve is normalized to its value at 300 K. In both panels, the $x = 0.17$ sample displays a monotonic evolution, as expected from the temperature dependence of its scattering

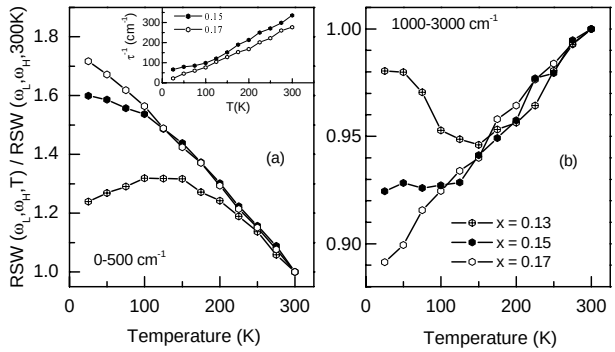

Fig. 3 – Temperature evolution of the restricted spectral weight. The integration boundaries ω_L–ω_H are indicated in each panel. The inset shows the dc extrapolation for the scattering rate for the $x = 0.15$ and 0.17 samples.

rate shown in the inset. The $x = 0.13$ sample displays a non-monotonic behavior in both frequency ranges. In panel (a) the increase of spectral weight due to the Drude narrowing is overcome at low temperatures by the gap opening. As expected, this trend is reversed in panel (b). For the $x = 0.15$ sample, the low ω *RSW* (panel (a)) shows at low T ($\lesssim 100\,\mathrm{K}$) a pronounced flattening relative to the $x = 0.17$ sample. The high ω *RSW* (panel (b)) shows the complementary effect: the decrease with decreasing T is halted below $T \approx 100\,\mathrm{K}$. On the other hand, the free-carrier scattering rate (inset) shows a smooth decrease over the whole temperature regime. This, combined with the clearly interpretable behavior of the $x = 0.13$ and 0.17 compounds, strongly suggests that a small gap opens below 100 K for $x = 0.15$. The experimental data show the presence of a normal-state partial gap in the materials with Ce concentration up to 0.15. To push our analysis further, a model to describe this gapped phase is necessary.

A natural interpretation is that the observed optical gap arises from commensurate (π, π) magnetic order. Neutron scattering consistent with this order has been unambiguously observed at lower dopings [22–24], but whether the order exists at superconducting concentrations is not yet settled. To investigate whether this physics can lead to the gap observed in our experiments, we have calculated the optical conductivity of a theoretical model of electrons moving in a band structure defined by the tight-binding dispersion appropriate to the cuprates [25, 26] along with a (π, π) density wave gap of magnitude $2\Delta_{SDW}$ (corresponding to the photoemission band splitting) and mean-field T-dependence. To calculate the conductivity, we evaluate the standard Kubo formula using the optical matrix elements appropriate to the tight-binding model and including in the electron propagators a frequency- and temperature-dependent self-energy with imaginary part increasing from a T-dependent dc limit (chosen to roughly reproduce $\rho(T)$ at $T < T_W$) to a weakly T-dependent high ω limit. The specific form chosen is $\Sigma(\omega, T) = i\gamma_0 + i\gamma_1[1 - \lambda(T)\omega_c(\omega_c - i\omega)/(\omega_c^2 + \omega^2)] - Z\omega$ with $\gamma_0 = 0.01\,\mathrm{eV}$, $\gamma_1 = 1.1\,\mathrm{eV}$, $Z = 0.4$, ω_c ranges from 0.15 eV at 300 K to 0.22 eV at low T and λ varies from 0.83 to 0.98 in the same temperature range. (A "marginal Fermi liquid" self-energy would have described the data almost as well, and leads to results very similar to those presented here.) As discussed in [26], we also included frequency and matrix element rescalings, by factors ~ 0.6 to account for high-energy (Mott) physics. Thus, the absolute values of σ should be regarded as estimates, but the relative frequency and temperature dependence as well as spectral-weight trends are expected to be reliable. The $x = 0.13$ calculated conductivities at 300 K and 25 K are compared to the measured values in the left panel of fig. 4. The calculation assuming a gap which opens at 170 K and saturates at a $T = 0$ value

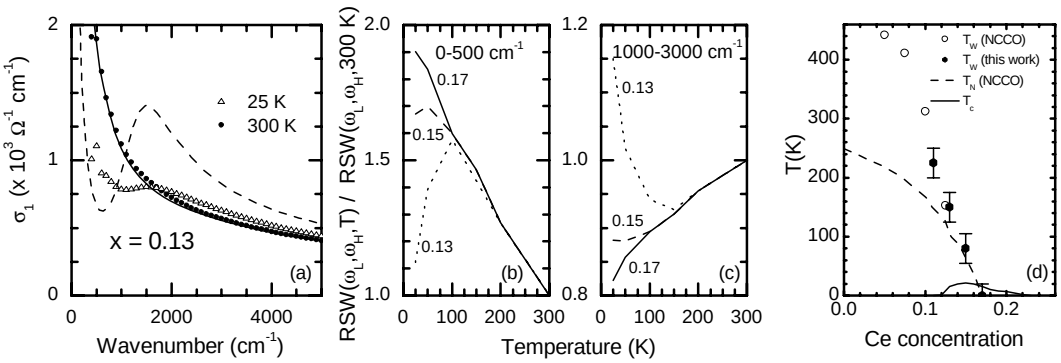

Fig. 4 – Panel (a): The symbols are the measured optical conductivity for $x = 0.13$ and the lines the spin density wave model calculation. Panels (b) and (c): RSW calculated for different dopings from the spin density wave model as described in the text. Panel (d): T_c and T_W, the temperature at which the optically defined gap opens (see text), *vs.* x. Open symbols are for NCCO from ref. [10], deduced from the maximum in $\sigma_1(\omega)$, and using the relation $\Omega_{Max}/k_B T_W = 14$. The dashed line shows T_N for NCCO from ref. [29].

$2\Delta_{SDW} = 0.25\,\mathrm{eV}$ is shown in the left panel of fig. 4 and resembles the measured conductivity. The two middle panels of fig. 4 show representative results of the modified spectral-weight analysis for three dopings ($x = 0.13$, $x = 0.15$ ($T_W = 70\,\mathrm{K}$, $2\Delta_{SDW} = 0.13\,\mathrm{eV}$) and $x = 0.175$ ($2\Delta_{SDW} = T_W = 0$)). It is evident that the calculation reproduces the different qualitative behaviors of the restricted spectral weight. In particular, the minimum in the high-frequency $RSW(T)$ curve corresponds to the opening of a gap. These curves therefore support the notion that the $x = 0.15$ sample in fact has a small density wave gap, although this is not directly visible in the measured optical spectrum, and further supports that the temperature at which the gap opens may be inferred from the position of the minimum or saturation in the RSW.

Detection of the gap by other means, especially via a low-energy spectroscopy which can probe the behavior as $\Delta \to 0$ in the $x = 0.15$–0.17 range, would be very desirable. Intriguing tunneling measurements [27,28] suggest the presence of a gap which is, however, much smaller and closes at much lower temperature than the one we find.

Figure 4(d) shows the gap onset temperature T_W obtained from the breakpoints in figs. 2 and 3, along with those extracted from optical measurements of NCCO by Onose *et al.* [10]. Also shown are the Néel temperature obtained from magnetic measurements on NCCO [29] and the superconducting transition temperature of the PCCO material studied here. The optically defined temperatures T_W are systematically higher than the magnetically defined T_N; we believe that this is a consequence of the very weak interplane coupling, which leads to a relatively wide "renormalized classical" regime in which two-dimensional thermal fluctuations suppress long-ranged magnetic order, but the spin correlation length and time are long enough for the fluctuations to produce a gap-like feature in the electronic spectrum.

The results reported here cover a large doping range up to the overdoped regime and strongly suggest that the T_W line ends at a critical concentration of $x \sim 0.17$ *well inside* the superconducting phase. Our interpretation implies the existence of two phases —a SDW and a Fermi liquid— and strongly suggests a QCP of magnetic origin, consistent with an interpretation based on dc transport in similar samples [15].

In conclusion, we have measured with great accuracy the reflectivity of electron-doped $Pr_{2-x}Ce_xCuO_4$ at various Ce doping levels (x). A careful optical conductivity spectral-weight analysis shows that a partial gap opens below a temperature T_W up to Ce concentrations of

$x = 0.15$. A spin density wave model reproduces satisfactorily the data where the gap has a clear spectral signature (for example, $x = 0.13$). The gap magnitude $2\Delta_{SDW}$ relates to T_W through $2\Delta_{SDW}/k_BT_W \sim 18$. T_W extrapolates to zero for $x \sim 0.17$, suggesting the presence of a quantum critical point inside the superconducting dome. We propose that, in at least one class of high-T_c superconductors, a normal-state gap is associated with an an ordered phase terminating in a QCP at approximately optimal doping. We hope these results will provide a point of reference which will help to resolve similar issues arising in the hole-doped materials.

* * *

The authors thank Dr. V. N. Kulkarni for RBS/Channeling measurements and Dr. P. Bassoul for electronic microcopy studies. The work at University of Maryland was supported by NSF grant DMR-0102350. The work at Columbia was supported by NSF contract DMR-0338376. The Work at Brookhaven National Laboratory was supported by DOE under contract DE-AC02-98CH10886.

REFERENCES

[1] Alloul H., Ohno T. and Mendels P., *Phys. Rev. Lett.*, **63** (1989) 1700.
[2] Takigawa M. *et al.*, *Phys. Rev. B*, **43** (1991) 247.
[3] Norman M. N. *et al.*, *Nature*, **392** (1998) 157.
[4] Puchkov A. V., Basov D. N. and Timusk T., *J. Phys. Condens. Matter*, **8** (1996) 10049.
[5] Santander-Syro A. F. *et al.*, *Phys. Rev. Lett.*, **88** (2002) 097005.
[6] Rice T. M. *et al.*, *J. Appl. Phys.*, **40** (1969) 1337.
[7] Grüner G., *Rev. Mod. Phys.*, **66** (1994) 1.
[8] Homes C. C. *et al.*, *Phys. Rev. B*, **56** (1997) 5525.
[9] Singley E. J. *et al.*, *Phys. Rev. B*, **64** (2001) 224503.
[10] Onose Y. *et al.*, *Phys. Rev. B*, **69** (2004) 024504.
[11] Lupi S. *et al.*, *Phys. Rev. Lett.*, **83** (1999) 4852.
[12] Armitage N. P. *et al.*, *Phys. Rev. Lett.*, **88** (2002) 257001.
[13] Fujita M., *Phys. Rev. B*, **67** (2003) 014514.
[14] Zimmers A. *et al.*, *Phys. Rev. B*, **70** (2004) 132502.
[15] Dagan Y. *et al.*, *Phys. Rev. Lett.*, **92** (2004) 167001.
[16] Maiser E. *et al.*, *Physica C*, **297** (1998) 15.
[17] Santander-Syro A. F. *et al.*, *Phys. Rev. B*, **70** (2004) 134504.
[18] McElroy K. *et al.*, *Nature*, **413** (2001) 282.
[19] Wissmann P. and Hummel R. E., *Handbook of Optical Properties*, Vol. **2** (CRC Press) 1997.
[20] Homes C. C. *et al.*, *Phys. Rev. B*, **66** (2002) 144511.
[21] Uefuji T. *et al.*, *Physica C*, **392-396** (2003) 189.
[22] Thurston T. R. *et al.*, *Phys. Rev. Lett.*, **65** (1990) 263.
[23] Matsuda M. *et al.*, *Phys. Rev. B*, **45** (1992) 12548.
[24] Yamada K. *et al.*, *J. Phys. Chem. Solids*, **60** (1999) 1025.
[25] Andersen O. K. *et al.*, *J. Phys. Chem. Solids*, **56** (1995) 1573.
[26] Millis A. J. and Drew H. D., *Phys. Rev. B*, **67** (2003) 214517.
[27] Biswas A. *et al.*, *Phys. Rev. B*, **64** (2001) 104519.
[28] Alff L. *et al.*, *Nature*, **422** (2003) 698.
[29] Mang P. K. *et al.*, *Phys. Rev. Lett.*, **93** (2004) 027002 and references therein.